Journal of Hydrology 669 (2026) 135088

Contents lists available at ScienceDirect

Journal of Hydrology

journal homepage: www.elsevier.com/locate/jhydrol

Sensitivity and scale dependence of discretization and roughness in the hydrodynamic modeling of surface runoff caused by torrential rainfall

David Feldmann[a,c,*], Patrick Laux[a,b], Andreas Heckl[c], Marinko Nujić[d], Brian Böker[c], Manfred Schindler[c], Harald Kunstmann[a,b]

[a] Karlsruhe Institute of Technology, Campus Alpin, Kreuzeckbahnstraße 19, Garmisch-Partenkirchen, 82467, Germany
[b] University of Augsburg, Institute of Geography, Alter Postweg 118, Augsburg, 86159, Germany
[c] Lindschulte Ingenieurgesellschaft mbH Ammersee, Billerberg 10, Inning am Ammersee, 82266, Germany
[d] IB-NUJIĆ j.d.o.o., 23F, Stari Laz, 51314, Croatia

HIGHLIGHTS

- Sources of sensitivities of hydrodynamic surface runoff modeling are identified.
- Depth-dependent roughness with high resolution increases discharge peaks by up to 20%.
- Constant roughness has no scale dependency effect.
- Change of surface resolution from 1 m to 4 m varies runoff peak by +−50%.
- Coarse models tend to create artificial depressions.

GRAPHICAL ABSTRACT

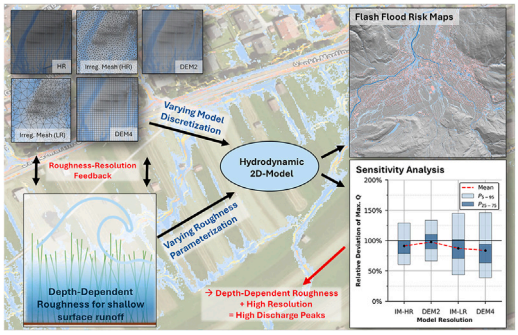

ARTICLE INFO

This manuscript was handled by Ashok Mishra, Editor-in-Chief, with the assistance of Giulia Sofia, Associate Editor

Keywords:
Model discretization
Depth-dependent roughness
Sensitivity analysis
Hydraulic rainfall-runoff modelling
Scale dependency
Surface runoff modelling
Flash floods

ABSTRACT

Hydrodynamic surface runoff simulations are an effective method for assessing flash flood risks. In engineering, the lack of observations for model calibration poses a challenge. Therefore, understanding the sensitivity to specific model parameters is crucial for reliable flood protection planning. This study analyzes how surface discretization and roughness affect surface runoff generation and depression storage in a hydrodynamic 2D-model in a southern German alpine region.

We compare the runoff generation across five discretization methodologies at 211 selected locations within the model domain. These locations are associated with subcatchments ranging in size from 0.2 to 4 km^2.

The discretization methodologies comprise a one-meter grid refined with survey data, a two-meter grid, a high-resolution and low-resolution irregular mesh and a four-meter grid. These are combined with seven different depth-dependent and constant roughness parameterizations.

The sensitivity analysis shows that a higher depth-dependent roughness is needed to achieve comparable results to those of a coarse resolution model. Significant differences were observed with varying roughness parameterizations and meshing approaches. Modest alterations to surface resolution have the potential to yield deviations of up to 20% in maximum runoff. Coarser resolution models tend to create artificial depressions, leading to unrealistic water storage on hillsides.

* Corresponding author at: Karlsruhe Institute of Technology, Campus Alpin, Kreuzeckbahnstraße 19, Garmisch-Partenkirchen, 82467, Germany.
Email address: david@gfeldmann.de (D. Feldmann).

https://doi.org/10.1016/j.jhydrol.2026.135088
Received 23 May 2025; Received in revised form 21 November 2025; Accepted 31 January 2026
Available online 2 February 2026

These findings aid in identifying the sources of sensitivity in hydrodynamic surface runoff modeling, especially in ungauged basins and provide guidance on specific model setups. This is particularly relevant given the continued use of coarse-resolution models due to computational constraints and the availability of various roughness parameterizations, while calibration data are scarce.

1. Introduction

The combination of climate change and urbanization exacerbates the risk of flash floods, which are triggered by intense rainfall overwhelming soil absorption capacity and leading to rapid surface runoff, even in areas distant from rivers (Fowler et al., 2021; Wilhelm et al., 2022). These events pose challenges due to their short warning times and can have devastating impacts (Borga et al., 2008). To mitigate such disasters, accurate information and preventive measures are crucial for authorities, communities, and individuals. Hydrodynamic models, particularly 2-dimensional ones, are instrumental in producing detailed hazard maps by simulating water flow paths and assessing vulnerable infrastructures (Bulti and Abebe, 2020). These models rely on numerical solutions of the shallow water equations and benefit from high-resolution topographic and LIDAR data, which allow precise terrain mapping (Luo et al., 2022).

Models are always a simplification of reality. Consequently, errors and uncertainties cannot be avoided. Uncertainties in hydraulic modeling arise from a lack of knowledge about boundary conditions, simplified processes, or parameter values, but also in observed data used to calibrate models (Beven et al., 2015). To enable end users to draw the right conclusions, the modeler must communicate the uncertainties (Teng et al., 2017). Although sensitivity analysis is common in science (Caviedes-Voullième et al., 2012; Fernández-Pato et al., 2016; Bellos et al., 2020; Costabile et al., 2023), it is often neglected in practical engineering due to lack of resources. Therefore, the engineer must be aware of model inherent sensitivities and where to expect them (Reinstaller et al., 2022).

Hydrodynamic surface runoff modeling exhibits sensitivity to four key factors. The first is the determination of rainfall input, which may involve using statistically derived return levels (Poschlod et al., 2021; Laux et al., 2023) or applying measurements of historical events (Vogl et al., 2022). Secondly, soil infiltration capacity plays a crucial role in determining the volume of surface runoff (García-Alén et al., 2023; Tügel et al., 2022). A third source of sensitivity is the resolution of the underlying surface model (Caviedes-Voullième et al., 2012; García-Alén et al., 2022). Finally, the parameterization of surface roughness is a critical factor that must be considered (Hou et al., 2018). Apart from the sensitivities caused by meteorological and hydrological parameters, the modeling technique of the hydrodynamic model is of paramount importance for the generation of robust results. This study focuses on how surface resolution affects model sensitivity and how it interacts with roughness parameterization.

The choice of surface roughness varies significantly between different surface properties. There are extensive collections of roughness coefficients in literature for larger water depths, such as those applied in riverine flood simulations (Chow, 1959). The most common way to apply roughness in hydraulic models is by using the Manning equation, which calculates surface drag using the empirically determined n-value. The use of land use-dependent friction can be considered a standard method for surface runoff modeling (Bellos et al., 2020; Fernández-Pato et al., 2016; Caviedes-Voullième et al., 2012) as well as for continental- and large scale studies (Alfieri et al., 2013).

An alternative to a single constant roughness parameter for each land use type is to use an explicit height approach to the water depth, often referred to as depth-dependent roughness (Hinsberger et al., 2022).

As shallow water depths play a significant role in heavy rainfall simulation, a depth-dependent formulation of roughness is a common approach in hydraulic surface runoff simulations (Gaur and Mathur, 2003; Rai et al., 2010; Mügler et al., 2011; Fraga et al., 2013; Özgen et al., 2015; Ye et al., 2018; Zhang et al., 2023). While some German water authorities (Altensell and Hoppe, 2022; Koch et al., 2016) set specific requirements for depth-dependent roughness coefficients, scientific literature provides a wider range of values (Wu et al., 1999; Fu et al., 2019; Hinsberger et al., 2022; Feldmann et al., 2023). In other guidelines and applications, it is recognized that the phenomenon of shallow surface runoff requires a distinct approach to roughness parameterization, differing from the methods typically employed in classical river hydraulics. However, due to model and data limitations, a constant approach is proposed (Babister and Barton, 2012; Rehman, 2011; Hall, 2015).

As roughness is strongly linked to the level of detail in the representation of the earth's surface, the model resolution is also a crucial source of sensitivity (Sauer and Ortlepp, 2021; David and Schmalz, 2021; Reinstaller et al., 2022; Caviedes-Voullième et al., 2012). High-resolution hydrodynamic models permit detailed simulations at the catchment scale by accounting for microscale flow affecting hydraulic structures, including walls, dams, and weirs (Macchione and Lombardo, 2021). Furthermore, the representation of small scale depressions is affected by the surface model resolution and meshing approaches employed, resulting in variations in the potentially stored water volume. (Jiang et al., 2023; Costabile et al., 2022; Marsh et al., 2018).

Despite recent advances in high-performance computing (HPC) (Costabile et al., 2023; Caviedes-Voullieme et al., 2023; Sanders and Schubert, 2019; Buttinger-Kreuzhuber et al., 2022; Tyrna et al., 2018), the majority of studies in engineering practice must achieve a balance between mesh resolution and computational effort (Sauer and Ortlepp, 2021; David and Schmalz, 2021; Reinstaller et al., 2022). Classical approaches employ local mesh refinements in accordance with topographic features (Hou et al., 2018; Savant et al., 2019; Marsh et al., 2018), while more advanced unstructured meshing methods adapt dynamically to evolving flows (Hu et al., 2019).

In their study, Caviedes-Voullième et al. (2012) compared the shallow surface runoff of locally refined triangular, right-angled, or grid-based meshes up to a maximum resolution of 5 m. They found that coarsening structured meshes results in a significant loss of topographic representation quality. Additionally, the use of unstructured meshes led to complex results depending on the meshing method employed. The best results were achieved with algorithms that refined the mesh at high terrain complexity. Furthermore, Caviedes-Voullième et al. (2012) conducted tests on various friction approaches, ranging from no friction to spatially uniform friction and a land-use-dependent definition. The use of friction resulted in significant damping of the hydrographs, as well as a reduction in mesh-dependent oscillations. The authors noted that the mesh resolution leads to mesh-dependent numerical friction, which requires individual calibration of physical friction depending on mesh resolution.

Another study (Sauer and Ortlepp, 2021) attempting to capture uncertainties in hydraulic flash flood modeling has demonstrated significant sensitivity to both, the model resolution and rainfall input. However, no strong variations in results could be determined related to roughness. It should be noted that Sauer and Ortlepp (2021) did not use a depth-dependent roughness parameterization. Furthermore, the authors found that even with coarse grids (10 m), areas prone to flooding could generally be determined. The main difference compared to finer grids is the variation of the inundation area. A clear effect of the model resolution on water depth and discharge could not be determined, as model output has been insufficient in this case.

The influence of roughness becomes more pronounced with longer flow paths. However, Sauer and Ortlepp (2021) suggest that future

studies should prioritize investigating sensitivity factors such as resolution and hydrology, as these may have a more substantial impact.

Reinstaller et al. (2022) attempted to identify sources of sensitivity in urban flood modeling. They concluded that roughness has a significant impact on the results, especially in steep catchments. Additionally, the authors recommend increasing roughness in hillside areas.

We evaluate how sensitivity to roughness and resolution varies within an uncalibrated model setup. To this end, we compare the hydrodynamically simulated runoff at 211 locations and their corresponding catchments across the model domain. The model domain is located in the municipality of Garmisch-Partenkirchen in southern Germany within the Alps. We apply five different model discretization strategies with different point densities and meshing approaches. These are combined with seven different roughness approaches, ranging from constant to depth-dependent.

By varying the model parameters of the hydrodynamic model and analyzing a large number of morphologically different catchments, we are able to identify general sources of sensitivity and interdependencies between resolution and roughness. For this purpose the catchments are classified according to their unit discharge patterns in hillslope and riverbed basins.

We demonstrate how a change in surface resolution affects the peak discharge and the depression storage volume. Furthermore, we investigate the sensitivities caused by the selection of a specific roughness approach. Finally, we show the interdependencies between roughness and resolution, particularly when a depth-dependent roughness approach is used. This will assist modelers in evaluating the uncertainties associated with model assumptions in ungauged study areas. The results also serve as a foundation to conduct robust model calibrations, since this requires knowledge about the parameter interdependencies of roughness and resolution.

2. Materials and methods

2.1. Study area

The municipality of Garmisch-Partenkirchen in Upper Bavaria, Germany, is chosen as the study area. This area is encompassed by alpine mountains, with some flat regions in the valley. The study area spans approximately 60 square kilometers and is situated at an elevation ranging from 671 to 1984 meters above sea level. Garmisch-Partenkirchen is prone to flooding caused by heavy rainfall in recent years (Kaiser et al., 2020) and will be affected by increased torrential rainfall intensities under climate change conditions (Laux et al., 2025). The topography is highly differentiated due to its alpine character, which allows the delineation of numerous subcatchments with different characteristics and sizes. Land use is divided into meadows and forests in the alpine parts of the area, while in the valley basin, meadows and sealed town areas predominate (CLMS, 2020a,b,c). This diversity of the area allows us to assess the generation of surface runoff under very different hydraulic conditions (Fig. 1).

A total of 211 locations (red dots in Fig. 1) and their corresponding catchments were analyzed to statistically evaluate surface runoff generation. Discharge is logged at the lowest point of each catchment in the hydrodynamic simulation. Subcatchments are delineated using GIS methods (Lindsay, 2014) and further refined by the simulated flow directions of the hydrodynamic simulation.

Table 1
Overview of the applied model resolutions, their data source, and the size of the model.

Name	Data	Tot. Nodes	Nodes/m^2	Max. Elem. Size
HR	regular grid (1 m) breaklines, terrestrial survey	60,484,642	1.01	1 m^2
IM-HR	Irregular Mesh based on DEM1, breaklines, terrestrial survey	20,778,014	0.35	16 m^2
DEM2	regular grid (2 m) based on HR-Model	15,238,347	0.25	4 m^2
IM-LR	Irregular Mesh based on DEM1, breaklines, terrestrial survey	3,979,590	0.07	200 m^2
DEM4	regular grid (4 m) based on HR-Model	3,809,592	0.06	16 m^2

2.2. Surface discretization

For the sensitivity analysis, five meshes are generated with different discretization approaches and data thinning methods (Table 1). The basic topographic data originates from LIDAR data and has been further processed and quality assessed by the Bayerische Vermessungsverwaltung (Bavarian Surveying Administration) (2024) into a regular grid or Digital Elevation Model (DEM) with a point distance of 1 m (DEM1).

The High-Resolution model (*HR-Model*) combines the DEM1 with additional survey data and breaklines from buildings and streets. To combine all these data, a framework has been developed to process the large amount of data. Since a regular grid with node distances of 1 m is not sufficient to represent all flow-affecting structures of the

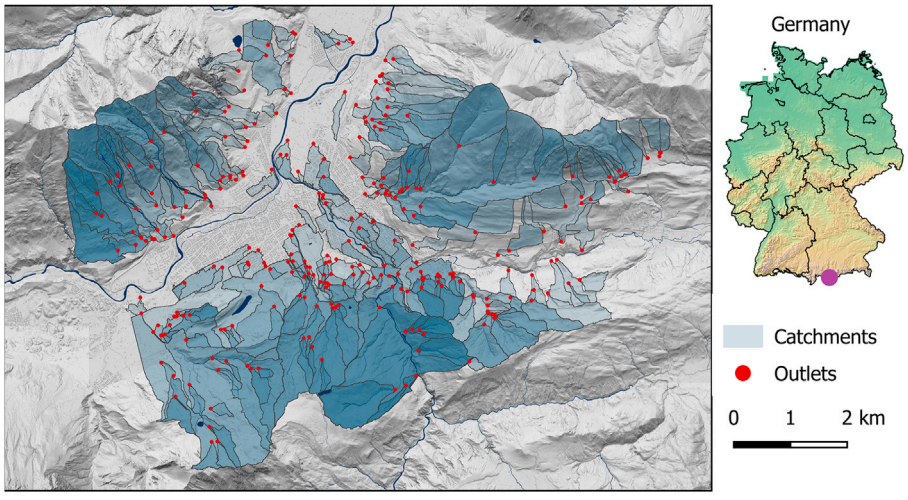

Fig. 1. Overview of the study area in Garmisch-Partenkirchen and the catchment boundaries, with their corresponding outlets, which were utilized for the evaluation of surface runoff generation. Geodata: Bayerische Vermessungsverwaltung (Bavarian Surveying Administration) (2024).

landscape, the developed framework can largely automate the generation of the mesh from different data sources. First, building perimeters with polygons from cadastral data are stamped into the mesh geometry to exactly represent the edges of buildings. To account for roof areas that contribute to runoff generation and to account for buildings as obstacles in the flow path, the interior of buildings is raised compared to the surrounding area. Second, in areas where a higher resolution is required, terrestrially surveyed points, lines, or surfaces are additionally integrated into the computational mesh. This is the case, for walls or curbstones that significantly influence potential flow paths. In addition, excavation pits that were present during the laser-scan flight must be revised subsequently. Third, existing terrestrially surveyed river models are obtained from local water authorities and integrated into the HR-Model. These surveyed models play a crucial role in accurately modeling riverbed discharge. This limitation arises from the nature of the DEM, which is derived from laser scan data that captures only the water surface, neglecting the topography of the riverbed. In addition, the geometries of special structures such as hydroelectric power plants, bridges, weirs, and culverts, having a significant influence on the runoff pattern within the city, can be taken from the river models. Therefore, this mesh achieves the highest possible resolution according to the availability of data (Fig. 2a). The HR-Model has been reused in the study of Laux et al. (2025).

Two Irregular Mesh Models with different point densities (*IM-LR-* and *IM-HR-Model*) are created based on the DEM1. The *IM-LR-Model* is created with the mesh generating software LASER_AS-2D 3.0, which is a standard commercial software for the creation of computational meshes for floodplains in Germany (Hydrotec, 2023). The software significantly reduces the original DEM data in the first step by generating a triangulated mesh with an element size of 20 to 30 m. In the second step, the mesh is refined with automatically generated 3D-breaklines, where a given height tolerance (Δz) is exceeded. In the present case, the default value of 0.2 m is applied. This ultimately results in a fine mesh in highly structured areas, while significantly reducing the amount of data in flat areas. Similarly to the HR model, buildings, surveyed structures and river models are also integrated into the mesh (Fig. 2b).

The *IM-HR-Model* is created using the mesh generator R_SIM (Nujić M, 2021). This software aims to generate high-resolution irregular meshes for floodplain simulations, since the increasing performance of modern CPUs, as well as improved parallelization and vectorization of state-of-the-art hydrodynamic models, allows for the fast computation of

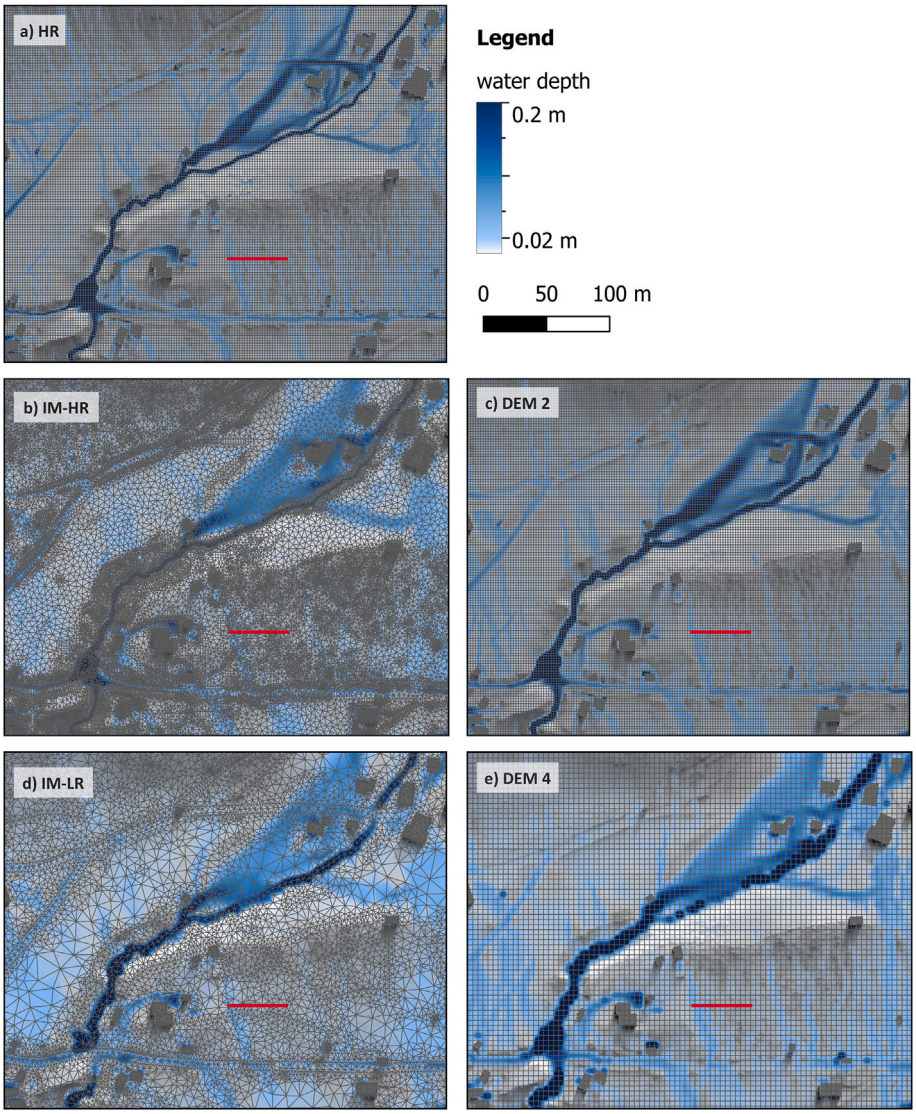

Fig. 2. Comparison of the mesh structure of the five surface discretization approaches of a randomly chosen hillslope. Blue areas indicate simulated flow paths with water levels above 0.02 m. Grey areas represent buildings. The red line shows the location of the cross-section in Fig. 3.

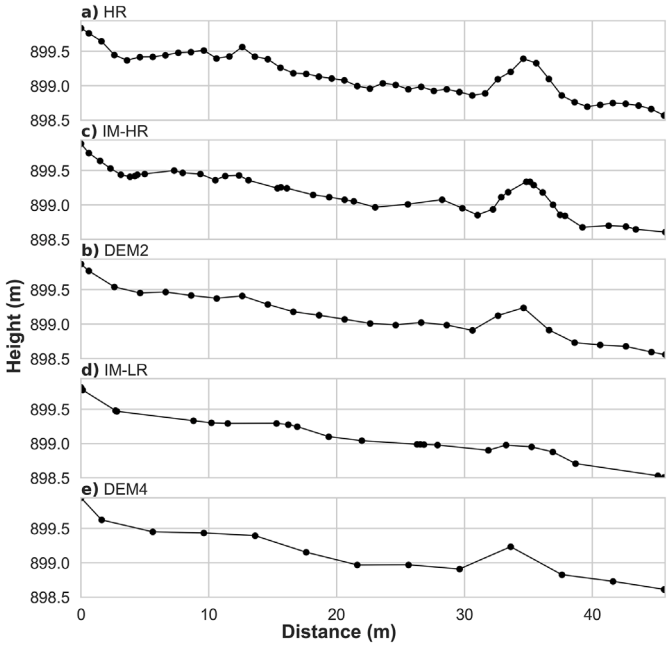

Fig. 3. Cross-sections of the topography of the meshes. The location is shown as a red line in Fig. 2.

large meshes. R_SIM selectively reduces the point density of the LIDAR data according to a given height tolerance. However, a much higher point density is preserved compared to LASER_AS-2D, depending on the strength of the terrain breaks, especially on dams and roads (Fig. 2c). Two regular grid digital elevation models with a point density of 2 m and 4 m (*DEM2* and *DEM4*) are created based on the HR-Model. Therefore, rivers, surveyed structures, and buildings are included as far as the model resolution of 2 m or 4 m can represent these structures. Unlike the other three models, the DEM consists entirely of a regular grid (Fig. 2d and e).

This ultimately leads to five meshes that differ essentially in the discretization of the topography (Figs. 2 and 3). Although hydraulically relevant structures such as rivers, buildings, or streets are modeled similarly, the resolution of remote terrain structures is strongly dependent on the chosen meshing method and therefore allows conclusions about its impact on surface runoff generation.

2.3. Effective rainfall

Hydrology is not part of the sensitivity analysis, as the scope of this work focuses on model discretization and roughness parameterization. However, a hydrological approach is needed to calculate the infiltration rate during the heavy rain event. The chosen hydrological approach applies to all conducted simulations. Rain is defined by so-called “source nodes” in the computational mesh. Consequently, each node has a particular rain quantity defined before initiating the simulation. For the sensitivity analysis, an event with a return period of 100 years and a duration of one hour is used. According to the KOSTRA2010R heavy precipitation statistical data set provided by the German Weather Service (DWD), this is 64 mm in 60 minutes for the study area (Junghänel et al., 2017).

The effective precipitation is calculated using a modified SCS-CN value method for South Germany (Kleeberg and Øverland, 1989; USDA National Resources Conservation Service, 2004) prior to the hydrodynamic simulation. The result is a time-invariant averaged runoff coefficient that varies spatially as a function of soil and land use.

The suitability of the SCS-CN value method for hydraulic heavy rain simulations is discussed in literature (Caviedes-Voullième et al., 2012). The principal benefit is that it is well-established and easily implemented. As the sensitivity analysis does not encompass hydrological parameters, this method is adequate for comparative purposes, although more sophisticated infiltration techniques, such as Green-Ampt, exist (Tügel et al., 2022). However, this would entail the introduction of further parameters, thereby increasing the complexity of the sensitivity analysis.

A constant rainfall, in conjunction with the constant infiltration approach derived from the applied SCS-CN Value method, results in stationary runoff conditions within small catchments, despite the employed approach for roughness or discretization. To circumvent the model’s tendency towards stationarity in small catchments, a center-weighted rainfall distribution (Deutscher Verband für Wasserwirtschaft und Kulturbau (DVWK), 1999), is implemented. This center-weighted rainfall distribution subdivides the design rainfall into three distinct intensity intervals, with the middle intensity being the highest.

2.4. Roughness

The application of depth-dependent roughness has been established in engineering practice for modeling surface runoff (Gaur and Mathur, 2003; Rai et al., 2010; Mügler et al., 2011; Fraga et al., 2013; Özgen et al., 2015; Ye et al., 2018; Zhang et al., 2023) and is meanwhile required by German water authorities as standard methodology (Koch et al., 2016; Altensell and Hoppe, 2022; Benson et al., 2024) for hydrodynamic heavy precipitation simulations. Literature provides a wide range of depth-dependent roughness measurements (Graf and Chhun, 1976; Wu et al., 1999; Fraga et al., 2013; Hinsberger et al., 2022) and parameterizations (Fu et al., 2019; Zhang et al., 2021; Feldmann et al., 2023). A selection of seven constant and depth-dependent roughness parameterizations oriented to values from literature is used to evaluate their impact on the generation of surface runoff (Table 2 and Fig. 4).

Table 2
Overview of the simulated scenario combinations between roughness parameterization and surface discretization.

Nr.	Approach	Source	HR	IM-HR	DEM2	IM-LR	DEM4
1	depth-dependent	Wu et al. (1999) Feldmann et al. (2023)	x	x	x	x	x
2	constant	Chow (1959) Brunner (2023)	x			x	
3	constant	maximum of scenario 1	x			x	
4	depth-dependent	scenario 1 decreased by 20%	x			x	
5	depth-dependent	scenario 1 increased by 20%	x			x	
6	depth-dependent	Koch et al. (2016) Altensell and Hoppe (2022) Hinsberger et al. (2022)	x			x	
7	constant	Engman (1986) Zeiger and Hubbart (2021) Tyrna et al. (2018)	x	x	x	x	x

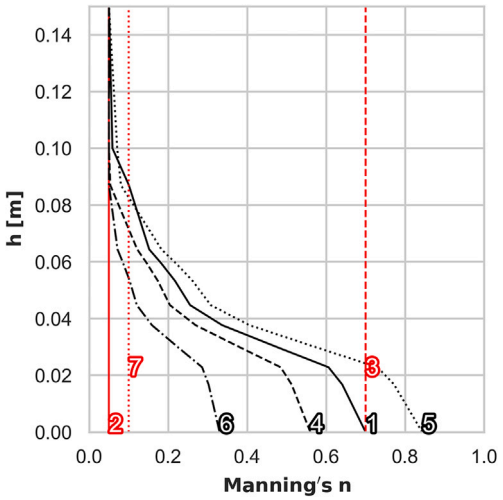

Fig. 4. Exemplary overview of the applied roughness curves of grassland and their corresponding scenario number, as shown in Table 2. The curves are represented in black for depth-dependent roughness and in red for constant roughness.

Scenario 1 uses a depth-dependent roughness parameterization oriented to values derived from Wu et al. (1999) and Feldmann et al. (2023), representing a dense vegetation.

In *Scenario 2*, constant Manning values are employed, which are typically utilized for fluvial flood simulations (Chow, 1959) and are also endorsed in the HEC-RAS 2D User's Manual (Brunner, 2023). It is important to acknowledge that these values are not advised for shallow overland flow, however, they are utilized in this study to demonstrate the impact of their application on the outcomes.

Scenario 3 uses the maximum roughness value of scenario 1, to demonstrate the effect of particularly high constant roughness.

Scenarios 4 and *5* use a depth-dependent approach and decrease or increase the surface roughness by 20% respectively compared to scenario 1 to test the sensitivity.

In *scenario 6* the depth-dependent roughness is further reduced by 50% compared to scenario 1. The applied values are in the range proposed by the German environmental authorities (Koch et al., 2016; Altensell and Hoppe, 2022). These values have been confirmed by Hinsberger et al. (2022) through laboratory experiments. According to Feldmann et al. (2023), this roughness function represents medium dense grasslands.

Scenario 7 employs a constant roughness approach, oriented to Manning values derived from field experiments for shallow overland flow (Engman, 1986). Similar constant Manning values have for example been used by Hinsberger et al. (2022), Zeiger and Hubbart (2021), and Tyrna et al. (2018). The values also represent a doubling of the constant roughness applied for water levels above 15 cm in scenario 1.

Based on empirical values (Chow, 1959; Altensell and Hoppe, 2022), we always assume a constant Manning value for water depths higher than 0.1 to 0.15 m for alpine meadows. This threshold depends in reality on the height of the vegetation and is therefore subject to a certain variation. Comparable thresholds for grassland are proposed in literature (Wu et al., 1999; Altensell and Hoppe, 2022; Koch et al., 2016; Hinsberger et al., 2022) and are in accordance with observations of vegetation height made in July on cultivated alpine meadows in the study area. Below this threshold, a depth-dependent approach is used in the scenarios 1, 4, 5, and 6. Sealed surfaces, such as roads or buildings, are completely modeled with a constant roughness due to the insignificant impact of a depth-dependent effect in such areas.

Table 2 shows an overview of all conducted simulation runs.

To represent the heterogeneity of the study area, data from different sources are used to define the surface roughness. CORINE Land Cover data with a resolution of 10 m is the basis for the roughness definition (Büttner, 2014). This data set distinguishes between tree density (0-100%) (CLMS, 2020c), degree of imperviousness (0-100%) (CLMS, 2020b), and other types of land use such as grasslands (CLMS, 2020a). As the spatial resolution of the CORINE Land Cover data is limited to 10 m, in areas where a more sophisticated definition of roughness values is required, precise polygons of buildings and streets can be taken from the official cadastral map. Each land use class such as grassland, forest, or street has its own roughness definition. The (depth-dependent) Manning value is interpolated linearly between 0% tree density (≡ grassland) and 100% tree density (≡ forest), as the data set provides a differentiated classification. For the degree of imperviousness, the same method can be applied. In this instance, the Manning value of grassland corresponds to a degree of surface sealing of 0%, whereas a degree of 100% is equivalent to that of a road which is then constant in every roughness scenario (see Fig. 5 and Table 3). The roughness of the riverbed is taken from calibrated river models from the local water authority.

2.5. Numerical hydraulic model

The calculation of non-stationary flow on a surface is usually solved using the two-dimensional depth-averaged flow equations, which are also often referred to as shallow water equations. They integrate Reynolds-averaged Navier-Stokes equations for incompressible fluids and the three-dimensional continuity equation over water depth, assuming a hydrostatic pressure distribution (Pironneau, 1988; Tan W. Y., 1992).

Applying the finite-volume method, the equations enable the calculation of water depth and flow velocity at each node of the computational mesh with a temporal resolution. As the study area consists of a computational mesh containing over 60 million points for the HR-Model, a fast solver for the shown equations is required. For this purpose, the 2D-hydraulic model H_SIM-2D offers significant advantages in terms of simulation time due to an implicit approach combined with effective parallelization and vectorization (Nujić M, 2023), allowing us to perform all simulation runs on a standard desktop computer.

The numerical solution method is based on the Fractional-Step method (Marchuk G, 1975). The time discretization uses the backward Euler method, which has been proven stable and accurate for non-stationary flow conditions (Ferziger et al., 2020). For instance, the time step of the HR model varies between 1.5 and 0.35 s. Convective fluxes are calculated with the aid of ENO (Essentially Non-Oscillatory) methods (Nujić, 1995; Shu and Osher, 1988) and streamline diffusion (Pironneau, 1988; Lafon and Osher, 1991). For the calculation of diffusive fluxes, a linear interpolation has been applied. In order to solve the governing flow equations, topography is discretized into a number of elements consisting of both triangles and quadrilaterals, as explained in Section 2.2. Consequently, the flexibility of H_SIM-2D permits the utilization of disparate model discretization methodologies, encompassing regular grids, irregular meshes, and combinations of both. In addition to adequate discretization in critical areas, mesh quality is a crucial factor. This entails generating a smooth mesh and avoiding acute or obtuse angles.

2.6. Quality assessment

The suitability of the results of each catchment for sensitivity analysis is evaluated according to a set of criteria. In certain instances, the discretization of the topography is inadequate. This is particularly evident in cases of lower-resolution models and extremely steep slopes. This leads to high Froude numbers (greater than 1.7) in the mean flow path, resulting in the formation of "Roll Waves" (Balmforth and Mandre, 2004). However, it is highly questionable whether the results of the model adequately reflect reality at this spatial and temporal resolution.

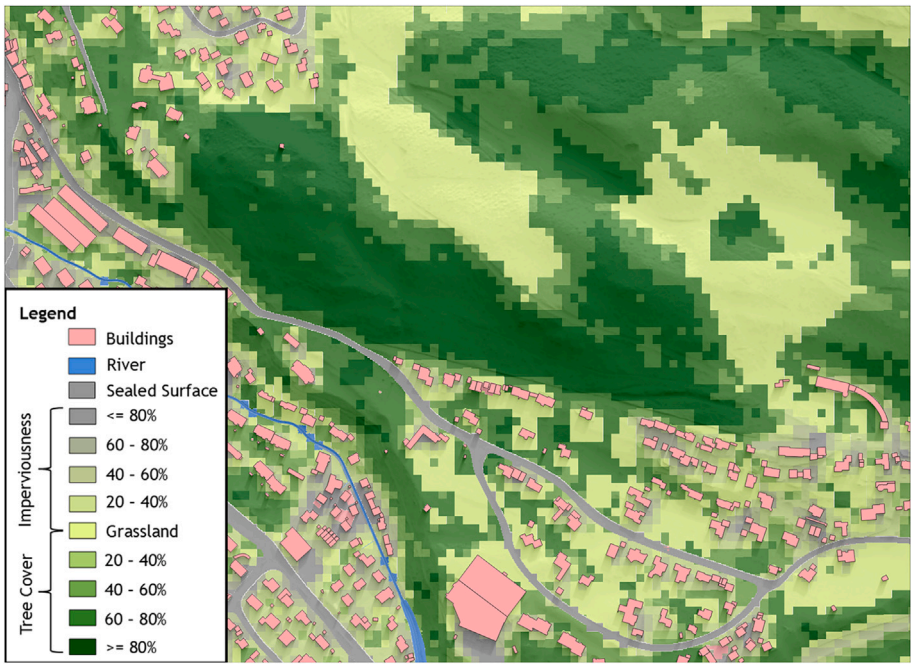

Fig. 5. Map section of the roughness defined in the model. The colors highlight the shift from a smooth surface (low imperviousness) to medium roughness (grassland) to high roughness (high tree cover).

Table 3
Manning's n for the main land-use types. The n-value is only valid above 0.15 m for the depth-dependent scenarios (1, 4, 5, 6).

Scenario	1	2	3	4	5	6	7
Sealed Surface (high imperviousness)	0.025	0.025	0.025	0.025	0.025	0.025	0.025
Grassland (low imperviousness and low tree cover)	0.05	0.05	0.7	0.05	0.05	0.05	0.1
Forest (high tree cover)	0.1	0.1	0.7	0.1	0.1	0.2	0.2

In situations where roll waves occur, the discharge becomes non-uniform due to the inherently non-steady nature of roll waves. Therefore, the hydrographs oscillate, leading to unreliable results and, consequently, their exclusion from the sensitivity analysis.

Second, the water balance of the catchment is verified. Thus, it is calculated whether the volume of the input rain (V_P) is equal to the runoff (V_q) plus the water in the catchment (V_h) (Eq. 1).

$$V_P = V_q + V_h \tag{1}$$

In case of an unsuccessful water balance check, the water potentially leaves the catchment through additional flow paths. These are typically caused by coarse discretization or depressions that overflow and drain in a different direction, which are not captured by the catchment delineation. In such instances, the results cannot be used for evaluation purposes and are therefore discarded.

Table 4 shows the number of catchments available for evaluation after the validity check.

The number of valid results increases with higher resolution due to enhanced numerical stability on steep slopes. The rise in usable results with higher and depth-dependent roughness should also be viewed in this context. A higher resolution also precludes cross-catchment flows due to inadequate representation of dam structures, which results in exclusion based on the volume check.

Table 4
Number of catchments that successfully pass the validity check for each simulation run.

Nr.	Roughness Approach	HR	IM-HR	DEM2	IM-LR	DEM4
1	depth-dependent	193	170	158	163	144
2	constant	133			113	
3	constant	178			152	
4	depth-dependent	180			157	
5	depth-dependent	188			165	
6	depth-dependent	188			158	
7	constant	177	149	147	153	130

2.7. Catchment classification

In order to evaluate different flow patterns between catchment types, a classification into riverbed and hillslope catchments is necessary. Hierarchical catchment classification according to hydromorphological properties has been applied in several studies (Rinaldi et al., 2013; Gurnell et al., 2016; Belletti et al., 2017).

To make a physically robust decision on the classification of catchments the unit discharge $[m^2/s]$ patterns of the HR-01 simulation run are evaluated based on a methodology proposed by Costabile et al. (2024). This method requires the calculation of the watershed drainage density

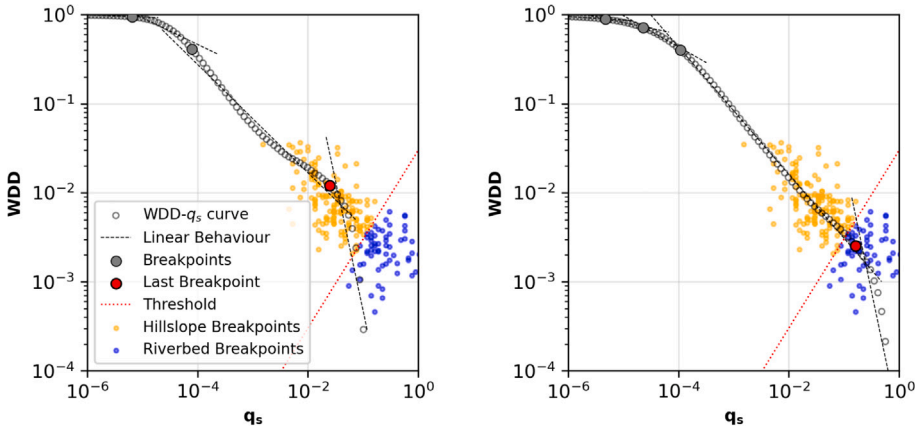

(a) WDD-q_s curve hillslope catchment (b) WDD-q_s curve riverbed catchment

Fig. 6. Log-log plot of WDD and q_s curve, showing the breakpoints derived through detection of linear behaviour (black dotted lines), indicating flow pattern changes and the position of the "last breakpoints" of all other catchments (orange and blue dots).

(WDD) as the ratio of hydrodynamically active cells (HAC) exceeding a given flow intensity threshold (q_s) to total catchment area (A).

$$WDD = \frac{\sum_{j=1}^{N} A_j}{A}, j \in HAC \tag{2}$$

$$HAC : \{q_i > q_s, i = 1 : N_{cel}\} \tag{3}$$

For any given value of q_s the area A_j of the hydrodynamic active cells (HAC) can be calculated. This relationship is analyzed as a log-log relation (see black circles in Fig. 6). The methodology is described in detail in Costabile et al. (2024).

Breakpoints (gray and red dots) in the log-log transformed WDD-q_s relationships are determined through a piecewise linear regression analysis (Pedregosa et al., 2012) with R^2 thresholds, minimum segment requirements for statistical robustness and slope ratio constraints to identify physically meaningful transitions in drainage behavior. Costabile et al. (2024) stated that the breakpoints represent the transition between flow patterns. In our use case, we identified the last breakpoint as reference for dividing the catchments into hillslope and riverbed catchments. In hillslope catchments, surface runoff is mostly diffuse and unchanneled, while in riverbed catchments, runoff is concentrated in a distinct flow path. To be able to analyze sensitivities for both catchment types, we divide the catchments at the red threshold line. It must be noted that this threshold must not be seen as a hard border, since the shift from shallow and diffusive overland flow to channeled runoff as the dominant flow process is fluid. The threshold line has been verified by a blind test of classifying the catchments according to their inundation areas.

3. Results

The results of 20 simulation runs of the whole model domain are evaluated. A thorough assessment of the inundation areas and hydrographs for each of the 211 subcatchments is conducted, contingent upon the successful completion of the validity check (Table 4). The subcatchments are classified into two categories based on their runoff patterns. Thus, the effect of depth-dependent roughness is more pronounced in hillslope catchments than in riverbed catchments. Mixed variants of the catchment types where flow patterns change unusually are generally excluded from the study because the factors influencing the results cannot be clearly distinguished.

3.1. Inundation areas and hydrographs

Fig. 7 shows exemplarily the maximum inundation areas of a small hillslope catchment, whose discharge is mainly unchanneled. The maps show more distinct flow paths with increasing resolution (Fig. 7a, d and e). A higher peak of the hydrograph correlates with a high model resolution. (Fig. 7b).

Fig. 8 shows a riverbed catchment whose runoff is concentrated along a distinct flow path. The relative differences in the runoff from the riverbed catchment are smaller compared to the hillslope catchment (Fig. 8b). These results can generally be observed in most riverbed catchments.

3.2. Maximum discharge

The risk posed by a flood wave can be most effectively represented by the maximum discharge, which reduces the results to a single value. To enable a cross-catchment comparison, we normalized the maximum discharge to the scenario with the highest model resolution as a reference. This deviation from a reference scenario is then evaluated in terms of model resolution and the roughness approach used (Fig. 9).

Fig. 9(a) shows the relative deviation of maximum discharge from the HR-model when using the depth-dependent roughness approach of scenario 1. The results demonstrate that the lower-resolution models (IM-LR, DEM4) exhibit an interquartile range (P_{25-50}) of the maximum discharge relative to the HR-model from 70% to 100% (IM-LR) and 55% to 90% (DEM4), while the mean deviation for both models is around 80%. The DEM2 and the IM-HR-model have a smaller interquartile range, but the mean deviation of the discharge (red line) is also reduced. With coarser resolution, this effect becomes even more pronounced (IM-LR and DEM4-model). We found no relative decrease in the maximum discharge using the constant roughness approach (Fig. 9b). Therefore, this effect must be caused by the depth-dependent roughness definition. To further investigate this phenomenon, we use the classification of hillslope and riverbed basins (Fig. 10) and compare the maximum discharge to the high-resolution model.

The evaluation of catchment classification demonstrates that hillslope catchments exhibit a diminished discharge maximum when using a coarser resolution, especially with the depth-dependent roughness approach. This effect is most pronounced in the IM-LR model. In this model, the point density of the mesh strongly depends on the terrain structure. The mesh generator increases point density near streams and valley floors, as breakline detection identifies topographic features and

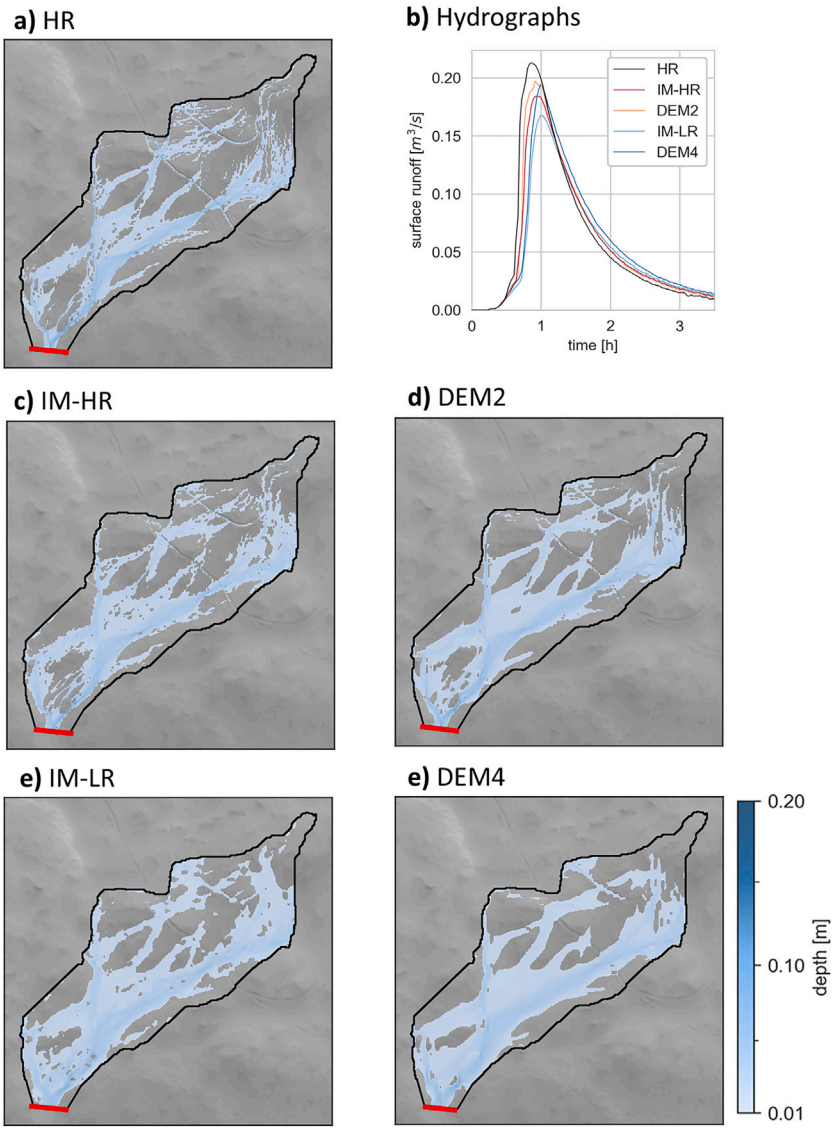

Fig. 7. Inundation areas of a randomly selected hillslope catchment and the related hydrographs of all five model resolutions for scenario 1. The red line marks the cross-section where the hydrographs are extracted.

automatically creates a continuous riverbed. Consequently, the mean deviation of maximum discharge in riverbed catchments is close to the results of the high-resolution model, although there is a high spread in the results. In contrast, the mean discharge of hillslope catchments in the IM-LR model is 20% lower compared to the high-resolution model. The reason for this behavior is illustrated in Fig. 11, which shows the minimum Manning's n value on a randomly selected hillslope during the simulation run of scenario 1, applying a depth-dependent roughness approach.

Manning's n-values correlate with water depth due to the depth-dependent roughness approach. Consequently, low n-values occur where water is concentrated in rills and flow paths. The plot clearly shows that low-resolution meshes fail to capture these rills, resulting in higher roughness as water is distributed over a larger area instead of accumulating. This distribution reduces flow velocity, leading to lower discharge peaks.

3.3. Depression storage

The application of disparate meshing methodologies leads to a spectrum of potential representations of depression storage within the surface model. In order to exclude the impact of roughness on the retention behavior, it is necessary to employ a scenario that utilizes a constant roughness approach. As the peak runoff of scenario 7 does not exhibit a discernible trend towards either a higher or lower maximum discharge (Fig. 9b), it serves as a sufficient example. The findings of the depression storage analysis are shown in Fig. 12, which depict the divergence between the maximum water volume compared to the HR-Model. The interquartile range ($P_{25} - P_{50}$) demonstrates a notable divergence in the water volume for coarse model resolutions (IM-LR: 96–110% and DEM4: 98–112%) compared to the HR model, with an average of around 105%. Moreover, the dispersion of hillslope catchments is more pronounced than that of riverbed catchments.

The increased storage volume of the coarser resolution models can be attributed to the presence of artificial obstacles within the flow paths. As illustrated in Fig. 8(f), an artificial retention volume is created as a consequence of inadequate mapping of flow paths. This phenomenon is not exclusive to water bodies; it can also be observed on minor flow paths on hillslopes, as evidenced by the lack of discernible differences in the mean value between catchment types. The irregular mesh of the IM-HR-model shows results that are closest to the HR-model, as it is able to

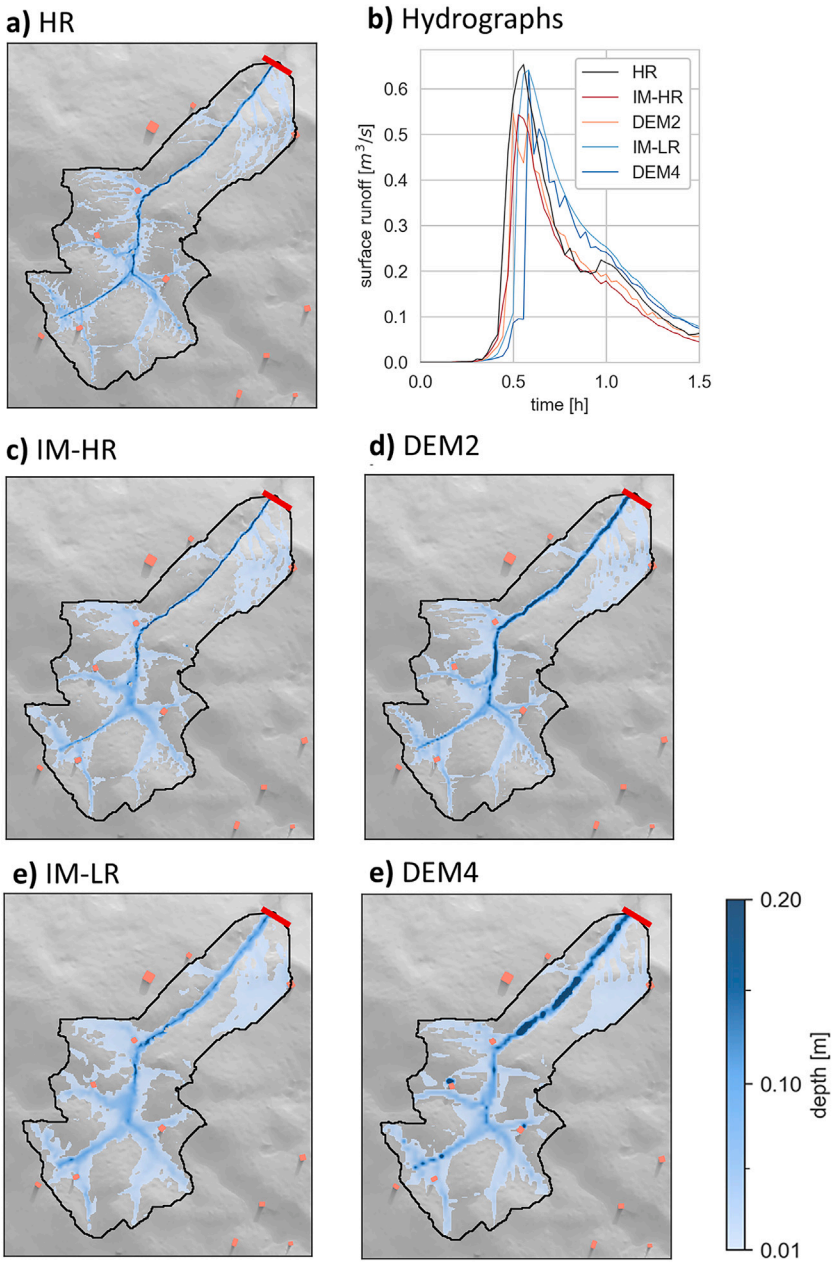

Fig. 8. Inundation areas of a randomly selected riverbed catchment and the related hydrographs of all five model resolutions for scenario 1. The red line marks the cross-section where the hydrographs are extracted.

represent flow structures in the elevation model and thus maintain high resolution where necessary.

3.4. Roughness parameterization

The sensitivity of the roughness parameterization of the HR and IM-LR-Model is now investigated. For this purpose, we compare the maximum discharge of the hillslope and riverbed catchments (Fig. 13).

Fig. 13(a) displays the relative deviation of the roughness scenarios from the HR-Model. The results indicate a notable dispersion, particularly evident in the divergence between the constant roughness approaches (scenarios 2, 3, 6 and 7) and the depth-dependent ones (scenarios 1 (reference scenario), 4, and 5).

Fig. 13(b) illustrates the results of the irregular mesh model IM-LR. The findings show that the mean deviation of the hillslope catchments is generally lower, while the mean deviation of riverbed catchments is similar to those of the HR-model. This phenomenon can be attributed to the fact that the impact of the depth-dependent roughness of scenario 1 in the IM-LR model is not as pronounced as that of the HR-model, as only this model is capable of capturing the intricate flow-affecting structures. Nevertheless, the high spread of results indicates that a coarse discretization can result in significant deviations from a higher-resolution model. Conversely, a high-resolution model is more susceptible to the impact of depth-dependent roughness. The comparison of the Fig. 13(a) and (b) also clearly shows that a high resolution leads to a smaller variability of peak discharge between the application of different roughness parameterizations.

4. Discussion

The simplification of roughness with Manning's n is a constant point of discussion (Lane, 2005; Ye et al., 2018; Hinsberger et al., 2022; Shen et al., 2023). In fluid mechanics, roughness is the reason for turbulent

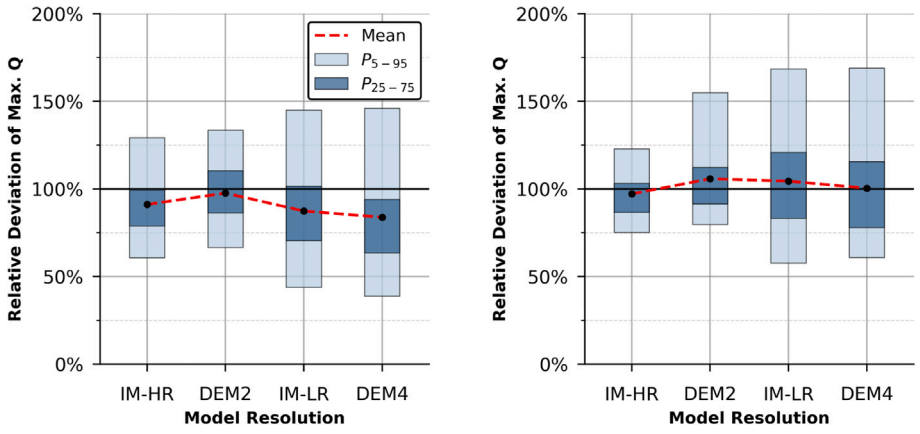

(a) Depth-dependent roughness (scen. 1) (b) Constant roughness (scen. 7)

Fig. 9. Relative deviation of the maximum discharge (Q) of all catchments from the HR-model.

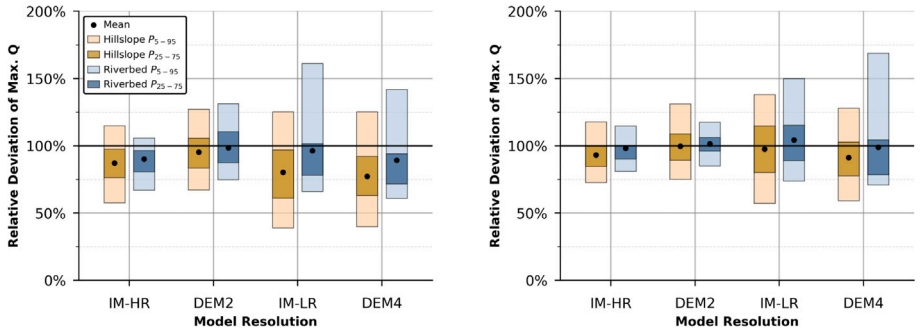

(a) Depth-dependent roughness (scen. 1) (b) Constant roughness (scen. 7)

Fig. 10. Relative deviation of the maximum discharge of hillslope and riverbed catchments (Q) from the HR-model.

flow which is then dissipated in the flow. With the depth-averaged flow equations, this cannot be resolved. Although the continuum mechanics and the Reynolds Averaged Navier Stokes formulae for turbulent flow consider implicitly all momentum and energy losses, a roughness parameterization is needed if the equation or discretization is simplified (Morvan et al., 2008). Lane (2005) argues that roughness is more a component of topography that has to be parameterized, rather than having any meaning in itself. The inconsistency in the way parameters are defined and the difficulty in establishing a universal scale for measurement make this subject particularly challenging. It is not possible to identify a single surface property that can be defined as 'the roughness'. Instead, roughness is a reflection of the precision of the measurement technique and the motivation for parameterization (Smith, 2014).

Therefore, roughness and topography are directly related and must be considered together. The results obtained substantiate this premise; it is imperative that the calculated roughness value encompasses all flow-affecting structures that are not represented within the employed mesh. It is therefore crucial to select the depth-dependent roughness in conjunction with the mesh resolution. Applying a constant roughness approach implies that a comprehensive representation of small-scale flow patterns is not within the scope of the simulation.

Hierarchical catchment classification (Brierley et al., 2013; Rinaldi et al., 2013; Belletti et al., 2017) can be used to further differentiate the catchments according to their flow patterns. Costabile et al. (2024) introduced a framework, suitable for 2D-hydrodynamic surface runoff simulations allowing the classification of catchments according to their unit discharge patterns. Based on this method the catchments are classified into hillslope and riverbed domains. The method is generally suitable for deriving additional or more detailed catchment classes. While shifting the threshold would change the absolute classification, the relative differences between scenarios remain interpretable.

Horritt et al. (2006) and Casas et al. (2010) state that a high model resolution will result in a reduction of roughness as geometric variability increases, thus reducing energy losses and partially replacing roughness parameterization. While this assumption is arguably sound, it is superseded by the effect of low roughness in small-scale flow paths due to the depth-dependent approach. Based on our results derived through the catchment classification process, a higher roughness would be required to achieve the same results as a coarser resolution model.

In addition it can be concluded that varying the return level and rain intensity will result in varying roughness resolution feedbacks in low model areas. Low rain intensities and a coarse model resolution will underestimate runoff, as lower water levels lead to a higher roughness. High resolution data potentially minimizes this effect.

This leads to the conclusion that a calibration of depth-dependent roughness functions with different model resolutions is necessary and is in accordance with the results of Caviedes-Voullième et al. (2012). Using small-scale roughness calibration from artificial slopes in a laboratory (Wu et al., 1999; Hinsberger et al., 2022) or from rainfall experiments (Ries et al., 2020; Feldmann et al., 2023) should consider the size of the calibrated obstacles.

Our results clearly show that the modeled discharge varies significantly between different model resolutions. This suggests that,

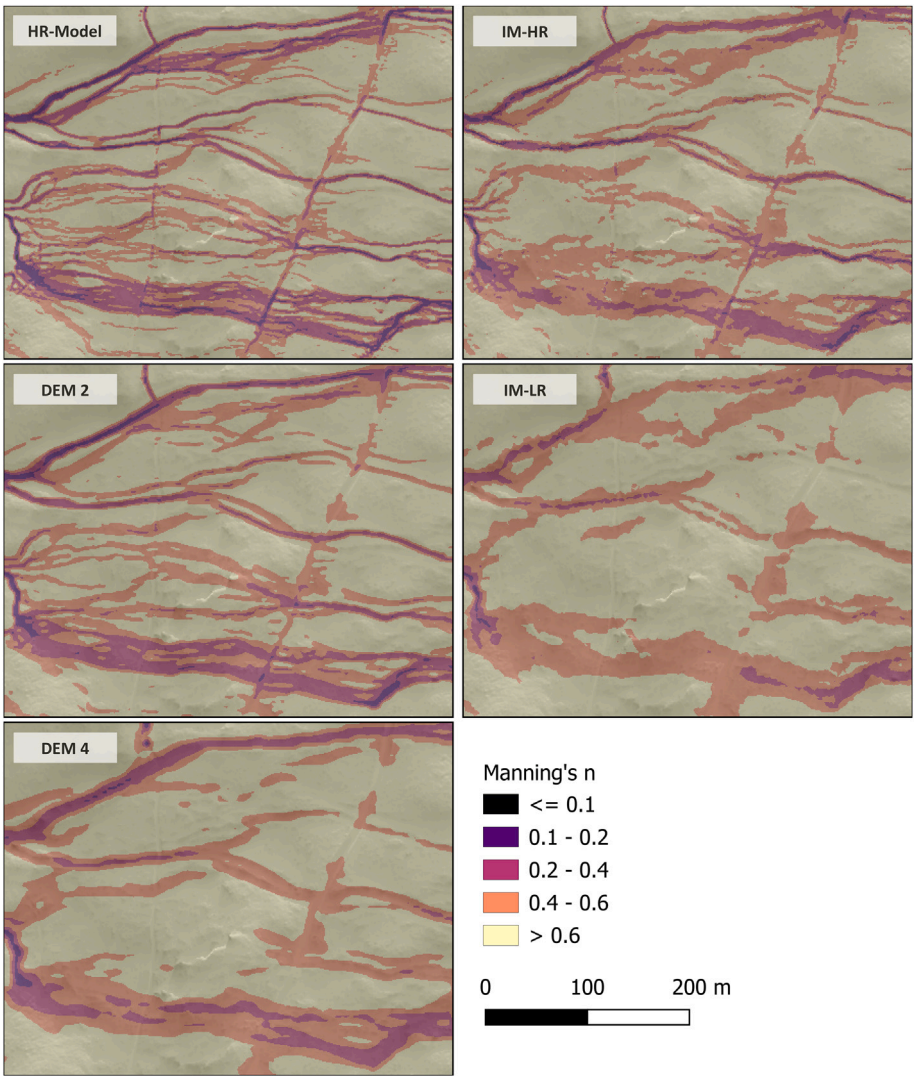

Fig. 11. Minimum Manning's n value on a randomly selected hillslope during the simulation run for scenario 1 (depth-dependent roughness).

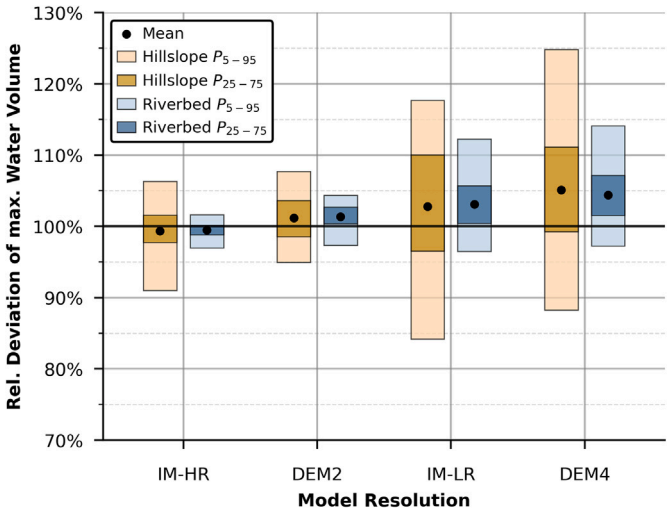

Fig. 12. Maximum water volume in the model during a simulation run between different mesh resolutions of scenario 7 (constant roughness) compared to the HR-Model.

if vegetation has been used for roughness determination through experiments, the model should accurately represent all features, such as rills and rocks.

The utilization of irregular meshes with local refinements in accordance with surface complexity represents a potential strategy for reducing data volume (Caviedes-Voullième et al., 2012; Marsh et al., 2018). However, this results in the loss of small flow-affecting terrain breaks on hillslopes, which are crucial when applying a depth-dependent roughness approach. Conversely, applying a constant roughness leads to similar results on average across mesh resolutions, although variability increases.

The use of hydrodynamic runoff simulations is becoming increasingly prevalent in the field of hydrology, replacing traditional models that do not adequately represent topographic depressions (Costabile et al., 2022; Barbero et al., 2022; Costabile et al., 2024). Consequently, the necessity for depression filling in flow routing (Jiang et al., 2023) has diminished, allowing for a more accurate representation of small-scale sinks and their impact on surface runoff generation. In light of the findings presented in this study, which indicate that coarse models can result in the creation of artificial depressions, this aspect must be taken into account. This is particularly important as virtual depressions reduce the volume of the hydrograph, while peak discharge may remain unaffected. Calculating

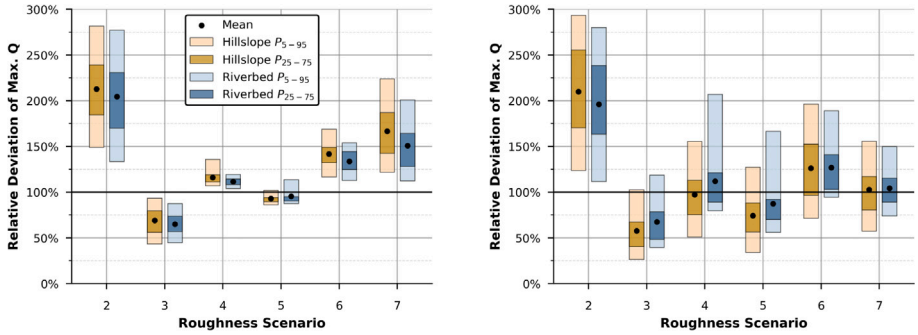

(a) HR-Model (b) IM-LR-model

Fig. 13. Relative deviation of the maximum discharge from scenario 1 of hillslope and riverbed catchments between different roughness scenarios (see Table 2).

the correct amount of water is essential when designing retention basins, for example.

The findings indicated that as the resolution increases, the variability of discharge generation decreases. This observation is particularly pertinent in the context of the growing availability of high-resolution LIDAR data exceeding 1 m. Further research is necessary to ascertain the resolution at which variability of surface runoff generation becomes negligible.

Calibration or validation of model parameters is crucial for reliable flash flood modeling. To determine robust roughness values with discharge data, the rain intensity and distribution and infiltration rate of the respective catchment must be considered, since these parameters influence each other (Bellos et al., 2020; Feldmann et al., 2023; Sun et al., 2025). This work provides a foundation for future model calibration efforts, as it shows the interdependency between resolution and roughness which is crucial when calibrating parameters that are valid beyond their respective study area.

5. Conclusions

Hydrodynamic simulations of heavy rainfall have proven highly effective in producing precise flash flood risk maps and supporting flood protection planning. However, model-inherent sensitivities must be taken into account when using these results for risk assessment, especially in ungauged areas where model calibration is not possible. In summary, the following key findings can be derived:

Impact of Resolution: The use of high-resolution surface discretization allows for a more precise representation of flood pathways. A reduction in the resolution through coarser grids or the use of terrain adapted irregular meshes leads to a possible variability in peak discharge generation from −50% to +50%.

Roughness-Resolution Feedback: Low-resolution models require lower depth-dependent Manning values to achieve discharge peaks comparable to high resolution models. This necessitates a tailored roughness calibration, as we observed an average 20% decrease in peak discharge for the lower-resolution models. This effect is not observable for constant roughness.

Depression Storage: On average, the examined models with coarser resolutions tend to store 5% more water by creating artificial barriers that impede water flow along both large and small paths.

The results reveal remarkable discharge variations due to different model resolutions, which are intensified by depth-dependent roughness. Since German water authorities require a depth-dependent roughness parameterization, it is crucial to consider this scale dependency in hydrodynamic flash flood simulations, especially as calibration data for surface runoff distant from gauged rivers is rarely available. These findings provide a basis for future model calibrations using real-world data.

CRediT authorship contribution statement

David Feldmann: Writing – original draft, Visualization, Software, Methodology, Conceptualization. **Patrick Laux:** Writing – review & editing, Supervision, Funding acquisition. **Andreas Heckl:** Writing – review & editing. **Marinko Nujić:** Writing – review & editing, Software. **Brian Böker:** Writing – review & editing. **Manfred Schindler:** Writing – review & editing, Supervision. **Harald Kunstmann:** Supervision, Project administration.

Declaration of competing interest

The authors declare that they have no known competing financial interests or personal relationships that could have appeared to influence the work reported in this paper.

Acknowledgement

This work was funded by the Bundesministerium für Forschung, Technologie und Raumfahrt (BMFTR) research project KARE (grant number 01LR2006D1).

Data availability

The authors do not have permission to share data.

References

Alfieri, L., Salamon, P., Bianchi, A., Neal, J., Bates, P., Feyen, L., 2013. Advances in pan-european flood hazard mapping. Hydrol. Process. 28, 4067–4077. https://doi.org/10.1002/HYP.9947

Altensell, N., Hoppe, H., 2022. Leitfaden Zur Aufstellung Von Konzepten Zum Kommunalen Sturzflut-Risikomanagement. Bayerisches Landesamt Für Umwelt (LfU), Augsburg.

Babister, M., Barton, C. (Eds.), 2012. Australian Rainfall & Runoff - Revision Project 15: Two Dimensional Modelling in Urban and Rural Floodplains. Barton.

Balmforth, N.J., Mandre, S., 2004. Dynamics of roll waves. J. Fluid Mech. 514, 1–33. https://doi.org/10.1017/S0022112004009930

Barbero, G., Costabile, P., Costanzo, C., Ferraro, D., Petaccia, G., 2022. 2D hydrodynamic approach supporting evaluations of hydrological response in small watersheds: implications for lag time estimation. J. Hydrol. 610, 127870. https://doi.org/10.1016/j.jhydrol.2022.127870

Bayerische Vermessungsverwaltung (Bavarian Surveying Administration), 2024. Geodata.

Belletti, B., Rinaldi, M., Bussettini, M., Comiti, F., Gurnell, A.M., Mao, L., Nardi, L., Vezza, P., 2017. Characterising physical habitats and fluvial hydromorphology: a new system for the survey and classification of river geomorphic units. Geomorphology 283, 143–157. https://doi.org/10.1016/J.GEOMORPH.2017.01.032

Bellos, V., Papageorgaki, I., Kourtis, I., Vangelis, H., Kalogiros, I., Tsakiris, G., 2020. Reconstruction of a flash flood event using a 2D hydrodynamic model under spatial and temporal variability of storm. Nat. Hazards 101, 711–726. https://doi.org/10.1007/S11069-020-03891-3/FIGURES/6

Benson, H., Neukum, H., Flasche, K., Delfs, M., Kausch, B., Fuchs, L., Iwannek, A., Scheer, H., Rieger, D., Rohlfing, R., Gerke, S., Henneberg, J., Andritschke, L., 2024. Kommunale Starkregenvorsorge in Niedersachsen - Praxisleitfaden Für Städte Und Gemeinden. Kommunale Umwelt-AktioN UAN E.V, Hannover.

Beven, K., Lamb, R., Leedal, D., Hunter, N., 2015. Communicating uncertainty in flood inundation mapping: a case study. Int. J. River Basin Manag. 13, 285–295. https://doi.org/10.1080/15715124.2014.917318

Borga, M., Gaume, E., Creutin, J.D., Marchi, L., 2008. Surveying flash floods: gauging the ungauged extremes. Hydrol. Process. 22, 3883–3885. https://doi.org/10.1002/HYP.7111

Brierley, G., Fryirs, K., Cullum, C., Tadaki, M., Huang, H.Q., Blue, B., 2013. Reading the landscape. Prog. Phys. Geogr. 37, 601–621. https://doi.org/10.1177/0309133313490007

Brunner, 2023. HEC-RAS 2D User's Manual. U.S. Army Corps of Engineers, Davis CA.

Bulti, D.T., Abebe, B.G., 2020. A review of flood modeling methods for urban pluvial flood application. Model. Earth Syst. Environ. 6, 1293–1302. https://doi.org/10.1007/s40808-020-00803-z

Buttinger-Kreuzhuber, A., Konev, A., Horváth, Z., Cornel, D., Schwerdorf, I., Blöschl, G., Waser, J., 2022. An integrated GPU-accelerated modeling framework for high-resolution simulations of rural and urban flash floods. Environ. Model. Softw. 156, 105480. https://doi.org/10.1016/J.ENVSOFT.2022.105480

Büttner, G., 2014. CORINE land cover and land cover change products. In: Remote Sensing and Digital Image Processing, vol. 18. Springer International Publishing, pp. 55–74. https://doi.org/10.1007/978-94-007-7969-3_5

Casas, A., Lane, S.N., Yu, D., Benito, G., 2010. A method for parameterising roughness and topographic sub-grid scale effects in hydraulic modelling from LiDAR data. Hydrol. Earth Syst. Sci. 14, 1567–1579. https://doi.org/10.5194/HESS-14-1567-2010

Caviedes-Voullième, D., García-Navarro, P., Murillo, J., 2012. Influence of mesh structure on 2D full shallow water equations and SCS curve number simulation of rainfall/runoff events. J. Hydrol. 448-449, 39–59. https://doi.org/10.1016/J.JHYDROL.2012.04.006

Caviedes-Voullieme, D., Morales-Hernandez, M., Norman, M.R., Ozgen-Xian, I., 2023. SERGHEI (SERGHEI-SWE) v1.0: a performance-portable high-performance parallel-computing shallow-water solver for Hydrology and environmental hydraulics. Geosci. Model Dev. 16, 977–1008. https://doi.org/10.5194/GMD-16-977-2023

Chow, V.T., 1959. Open Channel Hydraulics. McGraw-Hill, New-York.

CLMS, E.U.C.L.M.S, 2020a. CORINE land cover - grassland 2018 (raster 10 m), Europe. https://doi.org/10.2909/60639d5b-9164-4135-ae93-fb4132bb6d83

CLMS, E.U.C.L.M.S, 2020b. CORINE land cover - imperviousness density 2018 (raster 10 m), Europe. https://doi.org/10.2909/3bf542bd-eebd-4d73-b53c-a0243f2ed862

CLMS, E.U.C.L.M.S, 2020c. CORINE land cover - tree cover density 2018 (raster 10 m), Europe. https://doi.org/10.2909/486f77da-d605-423e-93a9-680760ab6791

Costabile, P., Costanzo, C., Gandolfi, C., Gangi, F., Masseroni, D., 2022. Effects of DEM depression filling on river drainage patterns and surface runoff generated by 2D Rain-on-Grid scenarios. Water 14, 997. https://doi.org/10.3390/W14070997

Costabile, P., Costanzo, C., Kalogiros, J., Bellos, V., 2023. Toward Street-Level nowcasting of flash floods impacts based on HPC hydrodynamic modeling at the watershed scale and High-Resolution weather radar data. Water Resour. Res. 59, e2023WR034599. https://doi.org/10.1029/2023WR034599

Costabile, P., Costanzo, C., Lombardo, M., Shavers, E., Stanislawski, L.V., 2024. Unravelling spatial heterogeneity of inundation pattern domains for 2D analysis of fluvial landscapes and drainage networks. J. Hydrol. 632, 130728. https://doi.org/10.1016/J.JHYDROL.2024.130728

David, A., Schmalz, B., 2021. A systematic analysis of the interaction between Rain-on-Grid-Simulations and spatial resolution in 2D hydrodynamic modeling. Water 13, 2346. https://doi.org/10.3390/W13172346

Deutscher Verband für Wasserwirtschaft und Kulturbau (DVWK, 1999. Hochwasserabflüsse. Bonn.

Engman, E.T., 1986. Roughness coefficients for routing surface runoff. J. Irrig. Drain. Eng. 112, 39–53. https://doi.org/10.1061/(asce)0733-9437(1986)112:1(39)

Feldmann, D., Laux, P., Heckl, A., Schindler, M., Kunstmann, H., 2023. Near surface roughness estimation: a parameterization derived from artificial rainfall experiments and two-dimensional hydrodynamic modelling for multiple vegetation coverages. J. Hydrol. 617, 128786. https://doi.org/10.1016/j.jhydrol.2022.128786

Fernández-Pato, J., Caviedes-Voullième, D., García-Navarro, P., 2016. Rainfall/runoff simulation with 2D full shallow water equations: sensitivity analysis and calibration of infiltration parameters. J. Hydrol. 536, 496–513. https://doi.org/10.1016/j.jhydrol.2016.03.021

Ferziger, J.H., Perić, M., Street, R.L., 2020. Computational Methods for Fluid Dynamics. Springer International Publishing,Cham,https://doi.org/10.1007/978-3-319-99693-6

Fowler, H.J., Lenderink, G., Prein, A.F., Westra, S., Allan, R.P., Ban, N., Barbero, R., Berg, P., Blenkinsop, S., Do, H.X., Guerreiro, S., Haerter, J.O., Kendon, E.J., Lewis, E., Schaer, C., Sharma, A., Villarini, G., Wasko, C., Zhang, X., 2021. Anthropogenic intensification of short-duration rainfall extremes. Nat. Rev. Earth Environ. 2 (2), 107–122. https://doi.org/10.1038/s43017-020-00128-6

Fraga, I., Cea, L., Puertas, J., 2013. Experimental study of the water depth and rainfall intensity effects on the bed roughness coefficient used in distributed urban drainage models. J. Hydrol. 505, 266–275. https://doi.org/10.1016/j.jhydrol.2013.10.005

Fu, S., Mu, H., Liu, B., Yu, X., Liu, Y., 2019. Effect of plant basal cover on velocity of shallow overland flow. J. Hydrol. 577, 123947. https://doi.org/10.1016/J.JHYDROL.2019.123947

García-Alén, G., González-Cao, J., Fernández-Nóvoa, D., Gómez-Gesteira, M., Cea, L., Puertas, J., 2022. Analysis of two sources of variability of basin outflow hydrographs computed with the 2D shallow water model iber: digital terrain model and unstructured mesh size. J. Hydrol. 612, 128182. https://doi.org/10.1016/J.JHYDROL.2022.128182

García-Alén, G., Hostache, R., Cea, L., Puertas, J., 2023. Joint assimilation of satellite soil moisture and streamflow data for the hydrological application of a two-dimensional shallow water model. J. Hydrol. 621, 129667. https://doi.org/10.1016/J.JHYDROL.2023.129667

Gaur, M.L., Mathur, B.S., 2003. Modeling Event-Based temporal variability of flow resistance coefficient. J. Hydrol. Eng. 8, 266–277. https://doi.org/10.1061/(asce)1084-0699(2003)8:5(266)

Graf, W.H., Chhun, V.H., 1976. Manning's roughness for artificial grasses. J. Irrig. Drain. Div. 102, 413–423. https://doi.org/10.1061/JRCEA4.0001116

Gurnell, A.M., Rinaldi, M., Belletti, B., Bizzi, S., Blamauer, B., Braca, G., Buijse, A.D., Bussettini, M., Camenen, B., Comiti, F., Demarchi, L., García de Jalón, D., González del Tánago, M., Grabowski, R.C., Gunn, I.D.M., Habersack, H., Hendriks, D., Henshaw, A.J., Klösch, M., Lastoria, B., Latapie, A., Marcinkowski, P., Martínez-Fernández, V., Mosselman, E., Mountford, J.O., Nardi, L., Okruszko, T., O'Hare, M.T., Palma, M., Percopo, C., Surian, N., van de Bund, W., Weissteiner, C., Ziliani, L., 2016. A multi-scale hierarchical framework for developing understanding of river behaviour to support river management. Aquat. Sci. 78, 1–16. https://doi.org/10.1007/s00027-015-0424-5

Hall, J., 2015. Direct rainfall flood modelling: the good, the bad and the ugly. Aust. J. Water Resour. 19, 74–85. https://doi.org/10.7158/13241583.2015.11465458

Hinsberger, R., Biehler, A., Yörük, A., 2022. Influence of water depth and slope on roughness—experiments and roughness approach for Rain-on-Grid modeling. Water 14, 4017. https://doi.org/10.3390/w14244017

Horritt, M.S., Bates, P.D., Mattinson, M.J., 2006. Effects of mesh resolution and topographic representation in 2D finite volume models of shallow water fluvial flow. J. Hydrol. 329, 306–314. https://doi.org/10.1016/J.JHYDROL.2006.02.016

Hou, J., Wang, T., Li, P., Li, Z., Zhang, X., Zhao, J., Hinkelmann, R., 2018. An implicit friction source term treatment for overland flow simulation using shallow water flow model. J. Hydrol. 564, 357–366. https://doi.org/10.1016/J.JHYDROL.2018.07.027

Hu, R., Fang, F., Salinas, P., Pain, C.C., Sto.Domingo, N.D., Mark, O., 2019. Numerical simulation of floods from multiple sources using an adaptive anisotropic unstructured mesh method. Adv. Water Resour. 123, 173–188. https://doi.org/10.1016/J.ADVWATRES.2018.11.011

Hydrotec, 2023. LASER_AS-2D - Reference Manual. Technical Report. www.hydrotec.de

Jiang, A.L., Hsu, K., Sanders, B.F., Sorooshian, S., 2023. Topographic hydro-conditioning to resolve surface depression storage and ponding in a fully distributed hydrologic model. Adv. Water Resour. 176, 104449. https://doi.org/10.1016/j.advwatres.2023.104449

Junghänel, T., Ertel, H., Deutschländer, T., 2017. KOSTRA-DWD-2010r Deutscher Wetterdienst: Bericht Zur Revision Der Koordinierten Starkregenregionalisierung Und -Auswertung Des Deutschen Wetterdienstes in Der Version 2010.

Kaiser, M., Borga, M., Disse, M., 2020. Occurrence and characteristics of flash floods in bavaria (germany). Clim. Change Manag. 293–310. https://doi.org/10.1007/978-3-030-37425-9_16

Kleeberg, H.B., Øverland, H., 1989. Zur Berechnung des effektiven oder abflußwirksamen Niederschlages. Mitteilungen des Instituts für Wasserwesen. Universität der Bundeswehr München 32, 19–62.

Koch, M., Hennegriff, W., Moser, M., Groteklaes, M., Krause, L., Röder, S., Gosch, L., Weinbrenner, D., Cassel, M., Wilkinson, K., 2016. Leitfaden Kommunales Starkregenrisikomanagement in Baden-Württemberg. LUBW Landesanstalt Für Umwelt Messungen Und Naturschutz Baden-Württemberg, Karlsruhe.

Lafon, F., Osher, S., 1991. High order filtering methods for approximating hyperbolic systems of conservation laws. J. Comput. Phys. 96, 110–142. https://doi.org/10.1016/0021-9991(91)90268-P

Lane, S.N., 2005. Roughness – time for a re-evaluation? Earth Surf. Process. Landf. 30, 251–253. https://doi.org/10.1002/ESP.1208

Laux, P., Feldmann, D., Marra, F., Feldmann, H., Kunstmann, H., Trachte, K., Peleg, N., 2025. Future precipitation extremes and urban flood risk assessment using a non-stationary and convection-permitting climate-hydrodynamic modeling framework. J. Hydrol. 661, 133607. https://doi.org/10.1016/J.JHYDROL.2025.133607

Laux, P., Weber, E., Feldmann, D., Kunstmann, H., 2023. The robustness of the derived design life levels of heavy precipitation events in the Pre-Alpine oberland region of southern Germany. Atmosphere 14, 1384. https://doi.org/10.3390/ATMOS14091384

Lindsay, J., 2014. The whitebox geospatial analysis tools project and open-access GIS. In: Proceedings of the GIS Research UK 22nd Annual Conference.

Luo, P., Luo, M., Li, F., Qi, X., Huo, A., Wang, Z., He, B., Takara, K., Nover, D., Wang, Y., 2022. Urban flood numerical simulation: research, methods and future perspectives. Environ. Model. Softw. 156, 105478. https://doi.org/10.1016/j.envsoft.2022.105478

Macchione, F., Lombardo, M., 2021. Roughness-Based method for simulating hydraulic consequences of both woody debris clogging and breakage at bridges in Basin-Scale flood modeling. Water Resour. Res. 57, e2021WR030485. https://doi.org/10.1029/2021WR030485

Marchuk, G., 1975. Methods of Numerical Mathematics, vol. 2. Springer-Verlag, New York.

Marsh, C.B., Spiteri, R.J., Pomeroy, J.W., Wheater, H.S., 2018. Multi-objective unstructured triangular mesh generation for use in hydrological and land surface models. Comput. Geosci. 119, 49–67. https://doi.org/10.1016/j.cageo.2018.06.009

Morvan, H., Knight, D., Wright, N., Tang, X., Crossley, A., 2008. The concept of roughness in fluvial hydraulics and its formulation in 1D, 2D and 3D numerical simulation models. J. Hydraul. Res. 46, 191–208. https://doi.org/10.1080/00221686.2008.9521855

Mügler, C., Planchon, O., Patin, J., Weill, S., Silvera, N., Richard, P., Mouche, E., 2011. Comparison of roughness models to simulate overland flow and tracer transport experiments under simulated rainfall at plot scale. J. Hydrol. 402, 25–40. https://doi.org/10.1016/j.jhydrol.2011.02.032

Nujić, M., 1995. Efficient implementation of non-oscillatory schemes for the computation of free-surface flows. J. Hydraul. Res. 33, 101–111. https://doi.org/10.1080/00221689509498687

Nujić, M., 2021. R_SIM Floodplain Mesh Generator - User Manual Version 1.0.

Nujić, M., 2023. H_sim-2D - the Model for Water Management - User Manual Version 1.8.

Özgen, I., Teuber, K., Simons, F., Liang, D., Hinkelmann, R., 2015. Upscaling the shallow water model with a novel roughness formulation. Environ. Earth Sci. 74, 7371–7386. https://doi.org/10.1007/s12665-015-4726-7

Pedregosa, F., Varoquaux, G., Gramfort, A., Michel, V., Thirion, B., Grisel, O., Blondel, M., Prettenhofer, P., Weiss, R., Dubourg, V., Vanderplas, J., Passos, A., Cournapeau, D.,

Brucher, M., Perrot, M., Duchesnay, E., 2012. Scikit-learn: machine learning in Python. J. Mach. Learn. Res. 12, 2825–2830. https://arxiv.org/abs/1201.0490v4

Pironneau, O., 1988. Finite Element Methods for Fluids. Wiley, Paris.

Poschlod, B., Ludwig, R., Sillmann, J., 2021. Ten-year return levels of sub-daily extreme precipitation over Europe. Earth Syst. Sci. Data 13, 983–1003. https://doi.org/10.5194/ESSD-13-983-2021

Rai, R.K., Upadhyay, A., Singh, V.P., 2010. Effect of variable roughness on runoff. J. Hydrol. 382, 115–127. https://doi.org/10.1016/j.jhydrol.2009.12.022

Rehman, H., 2011. Rainfall-on-Grid modelling - a decade of practice. In: 34th IAHR World Congress - Balance and Uncertainty, Brisbane.

Reinstaller, S., Krebs, G., Pichler, M., Muschalla, D., 2022. Identification of High-Impact uncertainty sources for urban flood models in hillside Peri-Urban catchments. Water 14, 1973. https://doi.org/10.3390/w14121973

Ries, F., Kirn, L., Weiler, M., 2020. Runoff reaction from extreme rainfall events on natural hillslopes: a data set from 132 large-scale sprinkling experiments in south-western Germany. Earth Syst. Sci. Data 12, 245–255. https://doi.org/10.5194/essd-12-245-2020

Rinaldi, M., Surian, N., Comiti, F., Bussettini, M., 2013. A method for the assessment and analysis of the hydromorphological condition of Italian streams: the morphological quality index (MQI). Geomorphology 180-181, 96–108. https://doi.org/10.1016/J.GEOMORPH.2012.09.009

Sanders, B.F., Schubert, J.E., 2019. PRIMo: parallel raster inundation model. Adv. Water Resour. 126, 79–95. https://doi.org/10.1016/j.advwatres.2019.02.007

Sauer, A., Ortlepp, R., 2021. Parameter uncertainties in flood hazard analysis of heavy rain events. ASCE-ASME J. Risk Uncertain. Eng. Syst. Part A: Civ. Eng. 7, https://doi.org/10.1061/AJRUA6.0001125

Savant, G., Trahan, C.J., Pettey, L., McAlpin, T.O., Bell, G.L., McKnight, C.J., 2019. Urban and overland flow modeling with dynamic adaptive mesh and implicit diffusive wave equation solver. J. Hydrol. 573, 13–30. https://doi.org/10.1016/J.JHYDROL.2019.03.061

Shen, E., Liu, G., Dan, C., Chen, X., Ye, S., Li, R., Li, H., Zhang, Q., Zhang, Y., Guo, Z., 2023. Estimating manning's coefficient n for sheet flow during rainstorms. CATENA 226, 107093. https://doi.org/10.1016/J.CATENA.2023.107093

Shu, C.W., Osher, S., 1988. Efficient implementation of essentially non-oscillatory shock-capturing schemes. J. Comput. Phys. 77, 439–471. https://doi.org/10.1016/0021-9991(88)90177-5

Smith, M.W., 2014. Roughness in the earth sciences. Earth-Sci. Rev. 136, 202–225. https://doi.org/10.1016/j.earscirev.2014.05.016

Sun, N., Huang, W., Creed, M., Sun, X., 2025. Impact of spatial distribution methods for rainfall on flash floods modelling using a hydrodynamic model. J. Flood Risk Manag. 18, e70010. https://doi.org/10.1111/JFR3.70010

Tan, W.Y., 1992. Shallow Water Hydrodynamics: Mathematical Theory and Numerical Solution for a Two-Dimensional System of Shallow Water Equations, 1 ed. Elsevier.

Teng, J., Jakeman, A., Vaze, J., Croke, B., Dutta, D., Kim, S., 2017. Flood inundation modelling: a review of methods, recent advances and uncertainty analysis. Environ. Model. Softw. 90, 201–216. https://doi.org/10.1016/j.envsoft.2017.01.006

Tügel, F., Hassan, A., Hou, J., Hinkelmann, R., 2022. Applicability of literature values for green–ampt parameters to account for infiltration in hydrodynamic rainfall–runoff simulations in ungauged basins. Environ. Model. Assess. 27, 205–231. https://doi.org/10.1007/S10666-021-09788-0

Tyrna, B., Assmann, A., Fritsch, K., Johann, G., 2018. Large-scale high-resolution pluvial flood hazard mapping using the raster-based hydrodynamic two-dimensional model FloodAreaHPC. J. Flood Risk Manag. 11, S1024–S1037. https://doi.org/10.1111/JFR3.12287

USDA National Resources Conservation Service, 2004. National Engineering Handbook: Part 630—Hydrology. U.S. Dep. Of Agric. Nat. Resour.Conserv. Serv.

Vogl, S., Laux, P., Bialas, J., Reifenberger, C., 2022. Modelling precipitation intensities from X-Band radar measurements using artificial neural networks—a feasibility study for the bavarian oberland region. Water 14, 276. https://doi.org/10.3390/W14030276

Wilhelm, B., Rapuc, W., Amann, B., Anselmetti, F.S., Arnaud, F., Blanchet, J., Brauer, A., Czymzik, M., Giguet-Covex, C., Gilli, A., Glur, L., Grosjean, M., Irmler, R., Nicolle, M., Sabatier, P., Swierczynski, T., Wirth, S.B., 2022. Impact of warmer climate periods on flood hazard in the european Alps. Nat. Geosci. 15 (2), 118–123. https://doi.org/10.1038/s41561-021-00878-y

Wu, F.C., Shen, H.W., Chou, Y.J., 1999. Variation of roughness coefficients for unsubmerged and submerged vegetation. J. Hydraul. Eng. 125, 934–942. https://doi.org/10.1061/(ASCE)0733-9429(1999)125:9(934)

Ye, A., Zhou, Z., You, J., Ma, F., Duan, Q., 2018. Dynamic manning's roughness coefficients for hydrological modelling in basins. Hydrol. Res. 49, 1379–1395. https://doi.org/10.2166/NH.2018.175

Zeiger, S.J., Hubbart, J.A., 2021. Measuring and modeling event-based environmental flows: an assessment of HEC-RAS 2D rain-on-grid simulations. J. Environ. Manag. 285, 112125. https://doi.org/10.1016/J.JENVMAN.2021.112125

Zhang, J., Zhang, S., Chen, S., Liu, M., Xu, X., Zhou, J., Wang, W., Ma, L., Wang, C., 2021. Overland flow resistance law under sparse STEM vegetation coverage. Water (Switzerland) 13, 1657. https://doi.org/10.3390/w13121657

Zhang, Y., Tügel, F., Han, H., Hou, J., Hinkelmann, R., 2023. Numerical investigation of depth-dependent roughness and infiltration methods in rainfall-runoff experiments. Urban Water J. 20, 652–664. https://doi.org/10.1080/1573062X.2023.2209061